Oxidative stress prediction: A preliminary approach using a response surface based technique

M. Sierra, L. Bragg-Gonzalo, J. Grasa, M.J. Muñoz, D. González, F.J. Miana-Mena

PII: S0887-2333(17)30313-2
DOI: doi:10.1016/j.tiv.2017.10.016
Reference: TIV 4147

Please cite this article as: M. Sierra, L. Bragg-Gonzalo, J. Grasa, M.J. Muñoz, D. González, F.J. Miana-Mena , Oxidative stress prediction: A preliminary approach using a response surface based technique. The address for the corresponding author was captured as affiliation for all authors. Please check if appropriate. Tiv(2017), doi:10.1016/j.tiv.2017.10.016

Oxidative stress prediction: a preliminary approach using a response surface based technique.

M. Sierra[a] , L. Bragg-Gonzalo[a] , J. Grasa[a], M. J. Muñoz[b], D. González[a], F. J. Miana-Mena,[a,*]

[a] *Applied Mechanics and Bioingeneering group (AMB). Aragón Institute of Engineering Research (I3A), University of Zaragoza, Spain*
[b] *Laboratorio de Genética Bioquímica (LAGENBIO). Facultad de Veterinaria. University of Zaragoza, Spain*

Keywords: Oxidative stress, Response surface, Lipoperoxidation, Oxidation rabbit organs, MDA + 4-HDA

[*] **Correspondence**: Professor Francisco J. Miana-Mena, Department of Pharmacology and Physiology, Facultad de Veterinaria, University of Zaragoza. C/Miguel Servet 177, 50013 Zaragoza, Spain. **e-mail**: *jmiana@unizar.es*.

1. Abstract

A response surface was built to predict the lipid peroxidation level, generated in an iron-ascorbate *in vitro* model, of any organ, which is correlated with the oxidative stress injury in biological membranes. Oxidative stress studies are numerous, usually performed on laboratory animals. However, ethical concerns require validated methods to reduce the use of laboratory animals. The response surface described here is a validated method to replace animals. Tissue samples of rabbit liver, kidney, heart, skeletal muscle and brain were oxidized with different concentrations of $FeCl_3$ (0.1 to 8 mM) and ascorbate (0.1 mM), during different periods of time (0 to 90 minutes) at 37ºC. Experimental data obtained, with lipid content and antioxidant activity of each organ, allowed to construct a multidimensional surface capable of predicting, by interpolation, the lipid peroxidation level of any organ defined by its antioxidant activity and fat content, when exposed to different oxidant conditions. To check the predictive potential of the technique, two more experiments were carried out. First, *in vitro* oxidation data from lung tissue were collected. Second, the antioxidant capacity of kidney homogenates was modified by adding melatonin. Then, the response surface generated could predict lipid peroxidation levels produced in these new situations. The potential of this technique could be reinforced using collaborative databases to reduce the number of animals in experimental procedures.

1. Introduction

The most important reactants in free radical biochemistry in aerobic cells are oxygen and its radical derivatives (superoxide and hydroxyl radical), hydrogen peroxide and transition metals which can provoke important alterations in all classes of biomolecules [1]. In order to avoid these processes, cells have developed antioxidant defence systems to help the organism to fight against free radical excess. They either scavenge and/or detoxify free radicals, block their production, sequester transition metals that are a source of donated electrons and stimulate antioxidant enzymes [2].

Oxidative stress has been described as a disturbance in the balance between the production of free radical and the antioxidant defences [3]. It is well established that increased oxidative stress in an organism causes damage to cellular membranes, lipid bilayers with embedded proteins that separates the eukaryotic cells from the extracellular environment. Its most abundant constituents are the phospholipids that formed the lipid bilayer [4]. This class of lipids could be affected by a degenerative chain reaction initiated by exposure to free radicals, resulting in peroxidation and formation of the peroxyl radical (*LOO**), endoperoxides and hydroperoxides [5]. Lipid hydroperoxides can break down into hydrocarbons, alcohols, ethers, epoxides and aldehydes. Two of this aldehydes are the malondialdehyde (MDA) and 4-hydroxy-alkenals (4-HDA), which can cross-link phospholipids, proteins and DNA. Because of this, many of the assay methods to determine free-radical injury in biological membranes are based on MDA concentration measurement [4].

Even if different organs present different susceptibility to oxidative-stress-induced injury, it is now known that oxidative stress is related to a large number of pathological conditions affecting all the organs [1, 6, 7, 8]. These diseases have been deeply studied with *in vivo* and *in vitro* models. Among the different causes which increase the oxidative stress, transitions metals, particularly iron, have been shown to contribute to many oxidative stress induced diseases [9, 10]. Via the

Fenton reaction, which requires a transition metal, H_2O_2 is converted to the devastatingly reactive hydroxyl radical (*HO**) provoking lipid peroxidation and mitochondrial dysfunction [11]. Thus, the *in vitro* model for induction of radical species via the Fenton reaction used a combination of $FeCl_3$ plus ascorbic acid and it is widely accepted in the field of oxidative stress research as an approximation to *in vivo* events [12, 13, 14].

Many of these works, *in vivo* and *in vitro*, are oriented towards the explanation and application of antioxidants to control disease development. Numerous experimental tests (*in vivo* or *in vitro*) are necessary to obtain satisfactory results with the consequent cost, not only economic but also in laboratory animals. Nowadays, because of several ethical concerns about animal experimentation, an important scientific challenge is to minimize the number of animals in experiments and replace them by validated methods [15, 16, 17].

In order to reduce the number of laboratory animals without interfering in the aims of the experimental investigation, the aim of this work was to generate a numerical model capable of predicting the quantity of lipid peroxidation of any organ when they are exposed to different oxidant conditions, including the presence of antioxidants, in an iron-ascorbate *in vitro* model. The mentioned numerical model is a response surface which needs minimal experimental information for its generation and once constructed, allows easy interpolations to obtain results with different combination of parameters. The response surface methodology (RS) has been applied in many works in the biomechanics and other biological fields [18, 19, 20, 21, 22] and it is based on multidimensional approximations that increase its complexity and computational cost depending on the number of variables considered. To reduce this order of complexity, the response surface methodology is combined in this work with the technology of model reduction, known as proper generalized decomposition (PGD) [23].

The principal goal is to develop a response surface that allows to predict the damage provoked to organs by oxidative stress. Basal *in vitro* oxidative stress level from different organs of rabbit (liver, brain, heart, kidneys and skeletal muscle) was determined. Then, these organs were subjected

to diverse oxidant conditions based on Fenton reaction, with different $FeCl_3$ concentrations and incubation times, obtaining a wide range of lipid peroxidation levels. As explained above, lipid peroxidation is related to lipid composition and antioxidant capacity, which were determined for each organ in order to include these variables in the numerical model and obtain a powerful and complete tool. Thus, the limits of this multidimensional surface would be determined by the oxidant conditions, lipid composition and antioxidant capacity of the organs.

Two additional experiments varying two of these variables (lipid composition and antioxidant activity) were carried out to check the predictive potential of the response surface previously developed. First, lung tissue, which was not previously used to develop our algorithm, was exposed to different oxidative environment. Second, kidney tissue was exposed again to the iron/ascorbate model, but its antioxidant activity was modified by adding an antioxidant agent. In both cases, the new parameters were compared with the mathematic results in order to validate the numerical model.

2. Material and Methods

2.1. Chemicals

$FeCl_3$, ascorbic acid, ethylenediamine-tetraacetic acid disodium (EDTA-Na_2), Tris (hydroxymethyl) aminomethane (TRIS), methanesulfonic acid and N-methyl-2-phenylindole were purchased from Sigma-Aldrich (Madrid, Spain). $FeCl_3$ and ascorbic acid were diluted in the incubation buffer (Tris-HCl 20 mM; pH 7.4). All reagents were prepared fresh just prior to use. Melatonin was diluted in absolute ethanol and the incubation buffer; the ethanol concentration was 2% (v/v) in the final mixture.

2.2. Animals and tissues homogenates

The handling and animal procedures were performed in strict compliance with the recommendations of the European Economic Community (86/609/CEE) for the care and use of laboratory animals. Twenty New Zealand Rabbits weighing around 2 kg were purchased from Servicio de Experimentación Animal (University of Zaragoza, Spain), and received standard food and water *ad libitum*. Animals were euthanized with intravenous sodium thiopental (50 mg/ kg) and perfused through the heart with 0.9% ice-cold saline, to minimize the excess of extracellular iron and other metallic ions. Immediately after perfusion, the different tissues (liver, kidney, heart, skeletal muscle, brain and lung) were quickly removed, washed in saline solution (0.9% NaCl), frozen, and stored at -80ºC prior to use.

2.3. Induction of oxidative damage in tissue homogenates

First, tissue samples of liver, kidney, heart, skeletal muscle and brain were weighed and homogenates were prepared using a glass homogenizer with ice-cold 20 mM TRIS (pH 7.4) at a final concentration of 1 g tissue / 5 ml of buffer. Then, lipid oxidation was induced by incubation of every tissue homogenate in a shaking water bath at 37ºC using five different concentrations of $FeCl_3$ (0.1, 0.5, 1, 5 and 8 mM) and ascorbate (0.1 mM). Each tube was duplicate and the number of samples was five for every organ and iron concentration. Moreover, a duplicate control sample of each tissue was incubated without iron or ascorbate. For every tissue and concentration, different incubation times were carried on. In all cases, samples were incubated in the water bath for 0, 10, 30, 60 or 90 minutes (n = 5 each). After incubating the samples as described above, the oxidative reaction was stopped by adding EDTA 2 mM and placing the aliquots on ice for 10 min. Then, they were centrifuged at 3,000 x g for 10 min at 4ºC. Thereafter, the supernatants were tested for their levels of MDA + 4-HDA concentrations.

Then, to validate the mathematical model developed, two additional experiences were made with different conditions to those previously described. First, lipid oxidation was provoked in a different tissue not used to build the response surface: lung. Lung homogenates were oxidized with 0.5 mM $FeCl_3$ and 0.1mM ascorbate concentrations for 30 minutes at 37ºC (n = 5 each), in this case $FeCl_3$ concentration and time duration were also randomly chosen. Second experiment, antioxidant activity (AA) of kidney homogenates were modified by adding different concentrations of melatonin (0.5 and 0.8 mM final concentration). The number of samples was five for each iron concentration. Melatonin is a non-enzymatic antioxidant that increase the AA of kidney homogenates. Then, lipid oxidation was induced by incubation with 0.5 mM $FeCl_3$ and 0.1 mM ascorbate concentrations for 30 minutes at 37ºC, $FeCl_3$ concentration and time duration were also randomly chosen.

2.4. Measurement of lipid peroxidation

The products of lipid peroxidation, MDA + 4-HDA, were measured in the tissue homogenates as explained before [24]. Briefly, tissue suspensions (200 μL) were mixed with 650 μL of a methanol:acetonitrile (1:3, v:v) solution containing N-methyl-2- phenylindole. After adding methanesulfonic acid (150 μL), incubation was carried out at 45ºC for 40 min. The MDA + 4-HDA concentrations were measured with a spectrophotometer at 586 nm using 4-hydroxy-nonenal as a standard. The level of lipid peroxidation in the homogenates was expressed as mmol of MDA + 4-HDA per gram of tissue.

2.5. Antioxidant activity

The ability of the homogenates to resist oxidative damage was determined as antioxidant activity, by ABTS assay [25]. Samples of tissue were homogenized in KCl 10% (w/v). Total antioxidant capacity

was quantified according to [25]. Summarily, 20 µL of biological sample or Trolox standard, was added to 2 mL of diluted $ABTS^{-+}$ solution, previously prepared. Then, the reaction was incubated for 6 minutes at 30ºC. The absorbance was determined at 6 min after initial mixing at 734 nm. The measurement of antioxidant activity of each tissue homogenate was replicated three times. The results are expressed as Trolox equivalents per gram wet tissue weight, i.e. the amount of Trolox (µmol) with an equivalent antioxidant potential to 1 g of the tissue under investigation.

2.6. Chemical analysis

Fat percentage was determined in different tissues (liver, kidney, heart, skeletal muscle, brain and lung) by ether extraction following Ankon method [26]. Moisture content was obtained by drying (103 ± 2ºC) to constant weight. Fat content is expressed in fat percentage of fresh tissue.

2.7. Statistical Analysis

Quantitative variables were defined by two parameters: arithmetic mean, as a measure of central trend, and standard error, as a dispersion measure. Before carrying out statistical analysis, data normal distribution was checked by a Kolmogorov-Smirnov test. Then, analysis of variance (ANOVA) were carried out and multiple comparisions among groups were performed by Scheffe tests. To demonstrate correlation between variables, a Pearson test was used. Standard statistical threshold was established at $p \leq 0.005$.

2.8. Response Surface Proper Generalized Decomposition methodology

Fitting techniques for high-dimensionless spaces are often very difficult to find and not easy to carry out due to its intrinsic complexities [27]. Traditional strategies for high-dimensional fitting

need to use high number of parameters that increase exponentially with the number of dimensions and the so-called "curse of dimensionality". However, model reductions techniques enable to work in high-dimensionless spaces avoiding this problem. In this work, we propose the use of a technique that combines the response surface methodology (RS) with model reduction known as Proper Generalized Decomposition (PGD) [28].

Briefly, response surfaces are multidimensional surfaces fit to quantities of interest, allowing easy interpolation to accomplish other realization with a different combination of parameters [29]. PGD is based on the use of separated representations and it was developed for solving multidimensional models [30, 31] and working in different stochastic modelling contexts [32]. The technique was extended to approach parametric models, where parameters were considered as model extra-coordinates. This made possible the calculation of the parametric solution, viewed as a computational vademecum, to be used for real-time simulation, optimization, inverse analysis and simulation-based control [33].

The PGD technique offers very good results in many fields where is applied, including biological models [34], dynamic problems [35], structural optimization [36], etc. Response surface approach has also been used in several works to study a wide range of biological processes such as drug delivery systems [37], biological production optimization [21, 20, 18, 38], nanoparticle studies [39, 40], etc.

Combining these two techniques, PGD and RSM, an approximation response function $f^{\mathrm{RSPGD}}(x_1 \ldots, x_n)$ is created to fit a data values' cloud coming from experiments. In our work, this response function depends on the values of 4 input variables or quantitative factors (fat composition of the organ, antioxidant capacity, $FeCl_3$ concentration and Incubation time) $\mathrm{x}= \{x_{\text{Fat Comp.}}, x_{\text{Antioxidant Cap.}}, x_{\text{Fe Concentration}}, x_{\text{Incubation time}}\}$ which are considered capable of defining a hyper surface in the bounden region (experimental region) $\Omega \subset \mathrm{R4}$, in which we consider constrained the values of **x** by the wide range of factors analyzed. This response surface has an output data that corresponds with the MDA + 4-HDA concentration solution.

In other words, we use a fitting technique that using a cloud of experimental data constructs a unique multi-parametric surface soluction of MDA + 4-HDA concentration $u_{MDA+4\text{-}HDA} = f^{\text{RSPGD}}(x_{\text{Fat Comp.}}, x_{\text{Antioxidant Cap.}}, x_{\text{Fe Concentration}}, x_{\text{Incubation time}})$ using 4 input data that correspond with fat composition, antioxidant capacity, $FeCl_3$ concentration and incubation time values.

The authors recommend to see their previous paper for a detailed description of the RSPGD methodology and its implementation [35]. Using this approach, we obtain that,

$$u_{\text{MDA+4-HDA}} = f^{\text{RSPGD}}(x_{\text{Fat Comp.}}, x_{\text{Antioxidant Cap.}}, x_{\text{Fe Concentration}}, x_{\text{Incubation time}}) = \sum_{i=1}^{\text{T}} \omega_{\text{i}} F_i^1(x_{\text{Fat Comp.}})$$

$$F_i^2(x_{\text{Antioxidant Cap.}})\, F_i^3(x_{\text{Fe Concentration}})\, F_i^4(x_{\text{Incubation Time}})$$

where T is the number of PGD modes obtained (usually less than 10), the functions F_i^k are computed using PGD classical approximation, k = 1,...,4 that correspond with fat composition, antioxidant capacity, Fe concentration and incubation time, respectively, and i= 1,..., T is the PGD modes index.

3. Results

First, the different rabbit tissue compositions and antioxidant capacities were characterized. These data were essential to develop the surface response afterwards.

3.1. Chemical Analysis

Fat percentage was determined in the different tissues (see Table 1). Brain was the tissue with the highest fat percentage (6.6%) whereas muscle had only 0.58%. Significant differences were found among all the tissues (p<0.05).

3.2. Antioxidant activity

The antioxidant activities of the different studied tissues are summarized in Table 1. Liver and kidney showed the highest antioxidant capacities (31.52 ±1.43 and 28.72 ± 0.36 Trolox equivalents), significantly greater than the other studied tissues (p<0.05).

Differences among brain, skeletal muscle and heart are not significant. As showed in Table 1, lung antioxidant capacity and fat content were determined to check the response surface potential but they were not included in the initial development of surface.

3.2.1. Computational procedure

In Figure 1 all the data for each time step where the MDA + 4-HDA concentration is known by experimental procedures are depicted. This is a cloud of 500 values [5(assays) × 4(time steps) × 5(organs) × 5($FeCl_3$ concentration)], that are into the experimental region, Ω, that is an hypervolume where the limits are [0.5, 7] x [18,32] x [0, 8.5] x [0, 95], for the different directions or parameters, fat, antioxidant activity, $FeCl_3$ concentration and time, respectively.

The simplest approach computed is depicted in Figure 2, where a linear approach of all data is obtained for the multi-parametric response surface. Regarding that $\mathbf{x} = (x_{\text{Fat Comp.}}, x_{\text{Antioxidant Cap.}}, x_{\text{Fe Concentration}}, x_{\text{Incubation time}}) \in \Omega = \prod_{i=1}^{4}[l_i, L_i]$, a linear response surface solution implies that all $F_i^k(x_k)$ will be linear functions, where again, k=1,...,4 corresponds with fat composition, antioxidant capacity, Fe concentration and incubation time, respectively and i =1,...,T is the PGD modes index. If all $F_i^k(x_k)$ are linear (using the simplest approach) a linear response surface $F(x_{\text{Fat Comp.}}, x_{\text{Antioxidant Cap.}}, x_{\text{Fe Concentration}}, x_{\text{Incubation time}})$ that fitting the data is obtained (2):

$$F(x_{\text{Fat Comp.}}, x_{\text{Antioxidant Cap.}}, x_{\text{Fe Concentration}}, x_{\text{Incubation time}}) = \sum_{i=1}^{T} \omega_i F_i^1(x_{\text{Fat Comp.}}) F_i^2(x_{\text{Antioxidant Cap.}}) F_i^3(x_{\text{Fe Concentration}}) F_i^4(x_{\text{Incubation Time}})$$

For the representation of the response surface solution, we employed a cloud of points defined in a mesh (representation mesh). These representation (or evaluation) meshes could have a lot of evaluation points. The coordinates of each evaluation point, represent different values of fat composition,

antioxidant capacity, Fe concentration and incubation time ant its color (the solution that offers the response surface) represents the MDA concentration.

Other different discretizations have also been employed. In Figure 3, a non linear response surface has been computed and represented: two elements for fat and antioxidant activity, four elements for $FeCl_3$ concentration and three for time are considered. In particular, $\{0.5,2.6,7\} \times \{18,20,32\} \times \{0,0.5,2.5,6.5,8.5\} \times \{5,35,65,95\}$ are used to divide the data in each direction.

To obtain the representation of Figure 2 and 3, we compute for all points, for the representation meshes, the value obtained for the response surface F using interpolation techniques in each direction (F_i^k, see [29] for more details).

3.3. Lipid Peroxidation and Response surface results

Lipid peroxidation levels and response surface results are presented together in order to visually explain the link between experimental and computational results organ by organ. The lipid peroxidation levels of each tissue were determined after its incubation at 37ºC for 10, 30, 60 and 90 minutes at different $FeCl_3$ concentrations. No significant differences were found between duplicates nor among the five independent repetition carried out at each time and concentration ($p>0.05$).

The response surface limits corresponded with maximum and minimum values of the different parameters taken into account to build the surface (MDA concentration, antioxidant activity, fat composition, $FeCl_3$ concentration and time). In order to obtain reliable data, all the results produced by this surface had to be within these limits.

Each tissue presents characteristic values of antioxidant capacity and fat and, if these two input data are setting for each organ, we obtain a particular solution of the response surface for different values of $FeCl_3$ concentration and for all the incubation times. Furthermore, several tests were made in order to check the behavior of the technique. The reference data used in these tests were an average of the experimental data.

The experimental results of lipid peroxidation are presented here for all the organs studied.

Liver MDA + 4-HDA values are summarized in Figure 4 (A). Lowest concentrations of $FeCl_3$ (0.1, 0.5 and 1 mM) provoked similar levels of lipid peroxidation ($p>0.05$) at any time. However, when the $FeCl_3$ was increased to 5 mM a variation was observed and from 60 minutes to the end, significant differences appeared with the highest concentrations described above ($p<0.05$). Furthermore, the highest $FeCl_3$ concentration (8 mM) caused raised values of lipid peroxidation from the very first incubation time (10 min). In fact, significant differences were observed between these values and all the other concentrations and times. The maximum level of lipid peroxidation was 753.24 ±105.09 nmol MDA/g of tissue at 8 mM of $FeCl_3$ and 90 min of incubation.

In Figure 4 (B), the response surface obtained for liver can be observed. For this case and for the rest of organs, a finer representation mesh has been used for a better understanding of the surface behavior. This particularization has been done setting the liver antioxidant capacity and fat values and obtaining the 3D representation on liver MDA + 4-HDA values through time. In order to check the model ability to predict the MDA + 4-HDA levels, liver average experimental data were compared to the predicted MDA + 4-HDA values. Five predictions, with different $FeCl_3$ concentrations and incubation times, are shown in Table 2. The deviation between experimental and predicted values varied from 0.5% to 15.9%. Not significant differences between experimental and predicted values were found ($p>0.05$).

The second organ analyzed was the kidney, whose MDA + 4-HDA results are shown in Figure 5 (A). Lipid peroxidation levels after incubation with the lower concentrations of $FeCl_3$ (0.1, 0.5 and 1 mM) showed significant differences with the control group at every time point ($p<0.05$). However, with 0.1 and 1 mM concentrations there were no significant differences among different incubation times ($p>0.05$) and with 0.5 mM, differences were observed between 90 min and the other incubation times. Highest concentrations (5 mM and 8 mM) showed significant differences with the other concentrations of $FeCl_3$. The maximum level of MDA + 4-HDA reached was 797.29 ± 42.41 nmol/g. In both organs, kidney and liver, the 8 mM oxidation curve seemed to acquire a similar pattern. Starting with high values at 10 min and quickly reaching a plateau from 30 min onwards

(p>0.05).

Figure 5 (B) shows the particularized surface for the kidney (antioxidant activity = 28.72 Trolox equivalents, and fat = 2.75%). MDA + 4-HDA concentration was predicted for every $FeCl_3$ concentration and time within the limits, as explained above. After checking the surface ability to predict MDA + 4-HDA concentration, deviations from 0.3% to 9.7% were obtained. In this case, not significant differences were observed between experimental and predicted values (p>0.05).

Heart and skeletal muscle were the next organs to be studied. Heart lipid peroxidation values are observed in Figure 6 (A). Lower concentrations (0.1, 0.5 and 1 mM) provoked similar amount of MDA + 4-HDA whereas with higher concentrations (8 mM), significant differences could be observed in all incubation times (p<0.05). The maximum value in this case was 1002.57 ± 72.08 nmol/g. At 5 mM, significant differences could be observed between 10 min oxidation and the control (p<0.05) however, with longer incubation times (30, 60 and 90 min), the oxidation level stabilized.

The particularized response surface for heart behavior is observed in Figure 6 (B). The prediction capability is shown in Table 2. The surface could accurately predict the MDA + 4-HDA values, showing deviations between 1.2% and 12.6%. No significant differences were obtained between experimental and predicted data (p>0.05).

In contrast to heart MDA + 4-HDA experimental values, muscle MDA + 4-HDA results were lower (see Figure 7 (A)). There was no difference among 0.1, 0.5, 1 and 5 mM. Hence, only 8 mM showed significant differences among the other values in all time points (p<0.05). Moreover, the maximum quantity of MDA + 4-HDA registered in muscle was 508.74 ± 51.85 nmol/g. The Figure 7 (B) shows the particular surface setting muscle antioxidant activity and fat content. Within the muscle limits, surface predicted the MDA + 4-HDA quantity with low deviations, from 0.6% to 6.5% (Table 2). No significant differences were found between experimental and predicted data (p>0.05).

Finally, brain MDA + 4-HDA levels are shown in Figure 8 (A). The lowest concentration (0.1 mM) provoked significant lipid peroxidation after 10-minute incubation, remaining constant at 30

and 60 minutes and finally increasing significantly again at 90 minutes (p<0.05). For the 0.5 mM and 1 mM $FeCl_3$ concentrations, the curve was very similar. In contrast, at 5 and 8 mM of $FeCl_3$ significant differences were observed (p < 0.05). In fact, the highest lipid peroxidation value of the experiment was reached in brain homogenates at 8 mM and 90 minutes: 1498 ±25.7 nmol/g. Figure 8 (B) shows the response surface obtained with brain antioxidant and fat characteristics. As it can be seen in Table 2, brain surface predicted MDA concentration with a deviation from 0.1% to 11.7%. Insignificant differences were observed between experimental and predicted values (p>0.05).

Since the main goal of this surface was to predict the lipid peroxidation of any combination of antioxidant activity and fat composition, we also carried out two more experiments to check the surface potential. First experiment was conducted to obtain MDA + 4-HDA experimental data from an organ not used on response surface building: lung. These data allowed us to check the deviation percentage, comparing predicted to experimental data. As explained above, lung antioxidant capacity and fat composition were determined and, with this information, the response surface was supposed to predict the MDA + 4-HDA level for $FeCl_3$ concentrations of 0.5 and 1 mM and 30 min, values randomly chosen. MDA experimental results, 91.30 ± 6.2 for 0.5 mM and 111 ±7.1 (nmol/g of tissue) for 1 mM, were correctly predicted by the response surface, showing a numerical MDA of 100.26 and 118.4 nmol/g of tissue, respectively. There were not significant differences between experimental and numerical results (p>0.05), validating the response surface to predict MDA levels even in organs not used to build the response surface

The goal of our response surface is also the prediction of lipid peroxidation in different conditions. Thus, the second experiment included a deeply studied antioxidant, melatonin. Melatonin addition to an organ homogenate increases its antioxidant capacity, modifying the results obtained by the surface. Knowing the antioxidant capacity increase provoked by melatonin, the response surface can predict the new values of lipid peroxidation. In order to test this capacity, different concentrations of melatonin (0.5 and 0.8 mM) were added to kidney homogenates, incubated with 0.5 mM $FeCl_3$ for 30 min, all the values were randomly chosen. Experimental

MDA values were 61.1 ± 8.3 and 57.9 ±5.4 (nmol/g of tissue) for 0.5 and 0.8 mM of melatonin, respectively. Predicted MDA values (70.2 and 59.3 nmol/g of tissue for 0.5 and 0.8 mM of melatonin), presented a maximum deviation of 14.9% and 2.4%. Not significant differences were found between experimental and predicted values ($p>0.05$), validating the response surface to predict MDA levels at any antioxidant activity.

4. Discussion

The main goal of this study was the development of a unique numerical response surface to predict the lipid peroxidation level of any tissue minimizing the experimental process. In the *in vitro* model presented here, the lipid peroxidation level of liver, kidney, skeletal muscle, heart and brain was determined under different conditions. They had different features that define their behavior against oxidative stress. This *in vitro* model is based on Fenton reaction, a basic and widely accepted model to induce oxidative stress [14]. Different $FeCl_3$ concentration (0.1, 0.5, 1, 5 and 8 mM) were chosen to provoke not only physiological but also pathological levels of oxidative stress. In this manner, the mathematical model could include a wider range of situations. Ascorbate concentration was fixed to 0.1 mM. Lowest concentration of $FeCl_3$ and ascorbate concentration were chosen from other previously developed studies [14, 41].

Data obtained from different organs were coherent with its different biological behaviors. Thus, liver and kidney possess an antioxidant capacity significantly higher than in other tissues ($p<0.05$) as a consequence of its exposition to a high amount of free radicals. Heart and muscle have the same antioxidant capacity (20%) but different fat percentage (3.6% and 0.58% respectively). It could explain the variations obtained in lipid oxidation values and behavior (600 nmol MDA + 4-HDA/ g muscle and 1000 nmol MDA + 4-HDA/g heart at the same time). The limited substrate on muscle homogenates would deplete sooner than heart substrate. Regarding the other studied organs, the maximum peroxidation value reached by the heart was higher than the liver and the kidney

(p<0.05), which could be justified by the bigger amount of fat plus the lower antioxidant activity with respect to these organs. Last but not least, brain has one of the lowest antioxidant capacities (20%) and the highest quantity of fat (more than 6%) which led to raised levels of MDA + 4-HDA (1500 nmol/g tissue at 8 mM and 90 minutes). Hence, it is the most sensitive tissue to oxidative stress, as the high number of neurological diseases related to it highlights [42].

In this study, each tissue was characterized by its antioxidant capacity and fat composition to take into account this two characteristics and not the tissue as a variable. Since the mathematical procedure pretended to create a unique response surface with the three different variables (fat content, antioxidant capacity and $FeCl_3$ concentration), it was important to determine a positive correlation between them. A Pearson test confirmed that there is a positive correlation between fat content and lipid peroxidation in any $FeCl_3$ concentration. This correlation is bigger with the highest concentrations (p<0.001 at 5 and 8 mM), reaching levels of R^2=0.981. This data could demonstrate that the oxidative damage caused at these conditions rely on the fat percentage of the tissue. Furthermore, the lipid peroxidation level shows a significant correlation (p<0.05) with antioxidant capacities only at low $FeCl_3$ concentrations (<[5mM]). Both cases suggest that, in this *in vitro* model, the antioxidant capacities of the tissue cannot control the oxidative stress after certain level. It is very likely that from that point onwards the oxidative stress level is no longer physiological. The correlation degree with the tissues fat, their antioxidant defences and oxidative damage indicates that the obtained results are viable and biologically coherent.

The unique multi-dimensional response surfaced created from the experimental data obtained in this study, is able to predict accurately by interpolation oxidative lipids damage of any tissue exposed to *in vitro* oxidation, with $FeCl_3$ and ascorbic acid within the tested conditions. Prediction accuracy improves with higher $FeCl_3$ concentrations and incubation times, as it could be observed in Table 2. Nevertheless, there were not significant differences between experimental and predicted values in any case. These results confirmed a powerful and validated tool that included a large number of situations and tissues, since the limits of $FeCl_3$ concentration and time were so wide (0 -

8 mM and 0 - 90 min respectively), as well as the antioxidant capacity and fat content (18.10 - 31.52 Trolox equivalents and 0.58 - 6.6%).

Therefore, this tool presents important advantages. First of all, the reduction of experiments and laboratory animals needed to carry out oxidative stress studies. To develop new studies, basic data about organs could be found in literature and data from antioxidant behavior would require a minimum number of experiments. Moreover, generally, on *in vitro* studies measuring oxidative stress, a fix number of points is determined to obtain the data [13, 9, 41]. Nevertheless, biological processes are continuous on time and information outside of the studied points is lost [22]. This response surface allows the acquirement of data of oxidative stress production and antioxidant action of any substance over time, in a continuous way.

On the one hand, since organs are only characterized here by its antioxidant capacity and fat content, we hypothesize that the response surface could predict lipid peroxidation from any organ independently of animal species, working inside the surface limits. To our knowledge, there are not published studies comparing tissues from different animal species subjected to in vitro oxidation under the same conditions. Moreover, fat content and antioxidant capacity of each organ are more similar among different species (e.g. rabbit muscle vs. rat muscle) than comparing different organs of the same species (e.g. rabbit muscle vs. rabbit brain). Since we demonstrated that our response surface predicts a wide range of different tissues, we hypothesize that this response surface could be used with tissues from other animal species, although further studies would be necessary.

On the other hand, this response surface also presents some limitations. Since surface's predictions are based on interpolations, input data (organ characteristics and oxidative conditions) should be placed inside the surface limits. Predictions based on input data placed outside of the surface limits should not be considered. In the future, these limits could be enlarged to improve the tool. Moreover, prediction obtained corresponds with lipid peroxidation of the tissue studied. In the future, this response surface could be complemented with other surfaces being able to predict protein oxidation, DNA damage,

membrane functional alterations, etc.

In conclusion, this multi-dimensional response surface is a first approach towards validating experimental models minimizing experiments and laboratory animals. Its usefulness relies on the ability to anticipate the effect of any intrinsic or added antioxidant activity without or with reduced empirical experiments. The most immediate application is the *in silico* screening of antioxidants and doses as a possible treatment for numerous diseases whose pathogenesis involves the oxidative stress. Moreover, this technique could be used to study and predict the oxidation level of different biomolecules such us proteins, DNA, etc.

5. Acknowledgments

The authors thank Professor José Álvaro Cebrián (Department of Molecular and Cellular Biology, University of Zaragoza, Spain) for the excellent technical advice and the facilities used in lipid oxidation experiments.

The work was financed by the University of Zaragoza under Young Researchers'14 program (project JIUZ-2014-BIO-05) and the predoctoral Grant of the Department of Industry and Innovation (Government of Aragón)

6. Conflicts of interest

The authors declare no commercial or financial conflict of interest

7. References

[1] P. Steinbacher, P. Eckl, Impact of oxidative stress on exercising skeletal muscle., Biomolecules 5 (2) (2015) 356–377. http://dx.doi.org/10.3390/biom5020356

[2] L. Fuentes-Broto, F. Miana-Mena, E. Piedrafita, C. Berzosa, E. Martínez-Ballarín, F. García-Gil, R. Reiter, J. García, Melatonin protects against taurolithocholic-induced oxidative stress in rat liver., J Cell Biochem 110 (5) (2010). 1219–1225. http://dx.doi.org/10.1002/jcb.22636

[3] D. Bonnefont-Rousselot, F. Collin, Melatonin: action as antioxidant and potential applications in human disease and aging., Toxicology 278 (1) (2010) 55–67. http://doi.org/10.1016/j.tox.2010.04.008

[4] J. J. García, L. López-Pingarrón, P. Almeida-Souza, A. Tres, P. Escudero, F. A. García-Gil, D.-X. Tan, R. J. Reiter, J. M. Ramírez, M. Bernal-Pérez, Protective effects of melatonin in reducing oxidative stress and in preserving the fluidity of biological membranes: a review., J Pineal Res 56 (3) (2014) 225–237. http://dx.doi.org/10.1111/jpi.12128

[5] M. T. Curtis, D. Gilfor, J. L. Farber, Lipid peroxidation increases the molecular order of microsomal membranes., Arch Biochem Biophys 235 (2) (1984) 644–649.

[6] F. J. Miana-Mena, C. González-Mingot, P. Larrodé, M. J. Muñoz, S. Oliván, L. Fuentes-Broto, E. Martínez-Ballarín, R. J. Reiter, R. Osta, J. J. García, Monitoring systemic oxidative stress in an animal model of amyotrophic lateral sclerosis., J Neurol 258 (5) (2011) 762–769. http://dx.doi.org/10.1007/s00415-010-5825-8

[7] M. Valko, D. Leibfritz, J. Moncol, M. Cronin, M. Mazur, J. Telser, Free radicals and antioxidants in normal physiological functions and human disease., Int J Biochem Cell Biol 39 (1) (2007) 44–84. http://doi.org/10.1016/j.biocel.2006.07.001

[8] M. J. Reiniers, R. F. van Golen, T. M. van Gulik, M. Heger, Reactive oxygen and nitrogen species in steatotic hepatocytes: a molecular perspective on the pathophysiology of ischemia-reperfusion injury in the fatty liver., Antioxid Redox Signal 21 (7) (2014) 1119–1142. http://dx.doi.org/10.1089/ars.2013.5486

[9] R. M. Uranga, N. M. Giusto, G. A. Salvador, Iron-induced oxidative injury differentially regulates PI3K/Akt/GSK3beta pathway in synaptic endings from adult and aged rats., Toxicol Sci 111 (2) (2009) 331–344. https://doi.org/10.1093/toxsci/kfp152

[10] E. Miller, A. Morel, L. Saso, J. Saluk, Melatonin redox activity. its potential clinical applications in neurodegenerative disorders, Current topics in medicinal chemistry 15 (2) (2015) 163–169. http://doi.org/10.2174/1568026615666141209160556

[11] R. J. Reiter, D. X. Tan, C. Osuna, E. Gitto, Actions of melatonin in the reduction of oxidative stress. a review., J Biomed Sci 7 (6) (2000) 444–458.

[12] E. Cadenas, M. G. Simic, H. Sies, Antioxidant activity of 5-hydroxytryptophan,5-hydroxyindole, and DOPA against microsomal lipid peroxidation and its dependence on vitamin E., Free Radic Res Commun 6 (1) (1989) 11–17.

[13] R. Tripathi, J. P. Kamat, Free radical induced damages to rat liver subcellular organelles: inhibition by andrographis paniculata extract., Indian J Exp Biol 45 (11) (2007) 959–967.

[14] S. Millán-Plano, E. Piedrafita, F. J. Miana-Mena, L. Fuentes-Broto, M.-B. E., L. López-Pingarrón, M. A. Sáenz, J. J. García, Melatonin and structurally-related compounds protect synaptosomal membranes from free radical damage., Int J Mol Sci 11 (1) (2010) 312–328. http://dx.doi.org/10.3390/ijms11010312

[15] M. M. Ciulla, G. Acquistapace, L. Toffetti, F. Magrini, R. Paliotti, Experimental animal models of myocardial damage in regenerative medicine studies involving adult bone marrow derived stem cells: ethical and methodological implications., Cardiovascular & hematological disorders drug targets 9 (2009) 86–94.

[16] R. B. M. de Vries, P. Buma, M. Leenaars, M. Ritskes-Hoitinga, B. Gordijn, Reducing the number of laboratory animals used in tissue engineering research by restricting the variety of animal models. articular cartilage tissue engineering as a case study., Tissue engineering. PartB, Reviews 18 (2012) 427–435. URL http://dx.doi.org/10.1089/ten.TEB.2012.0059

[17] H. Behrensdorf-Nicol, B. Krämer, [reduction of animal experiments in experimental drug testing]., Bundesgesundheitsblatt, Gesundheitsforschung, Gesundheitsschutz 57 (2014) 1173–1180. http://doi.org/10.1007/s00103-014-2033-1

[18] N. IA Haddad, H. Gang, J. Liu, S. Maurice Mbadinga, B. Mu, Optimization of surfactin production by bacillus subtilis hso121 through plackett-burman and response surface method, Protein and peptide letters 21 (9) (2014) 885–893.

[19] V. S. Nirmalanandhan, J. T. Shearn, N. Juncosa-Melvin, M. Rao, C. Gooch, A. Jain, G. Bradica, D. L. Butler, Improving linear stiffness of the cell-seeded collagen sponge constructs by varying the components of the mechanical stimulus., Tissue Eng Part A 14 (11) (2008) 1883–1891.
http://dx.doi.org/10.1089/ten.tea.2007.0125

[20] R. Kaushik, S. Saran, J. Isar, R. Saxena, Statistical optimization of medium components and growth conditions by response surface methodology to enhance lipase production by aspergillus carneus, Journal of Molecular Catalysis B: Enzymatic 40 (3) (2006) 121–126. http://doi.org/10.1016/j.molcatb.2006.02.019

[21] R. Muralidhar, R. Chirumamila, R. Marchant, P. Nigam, A response surface approach for the comparison of lipase production by candida cylindracea using two different carbon sources, Biochemical Engineering Journal 9 (1) (2001) 17–23.

[22] K. Sun, G. F. Krause, F. L. Mayer, M. R. Ellersieck, A. P. Basu, Estimation of acute toxicity by fitting a dose-time-response surface, Risk Analysis 15 (2) (1995) 247–252.

[23] F. El Halabi, D. González, A. Chico, M. Doblare, FE2 multiscale in linear elasticity based on parametrized microscale models using proper generalized decomposition, Comput. Meth. Appl. Mech. Eng. 257 (2013) 183–202.
http://doi.org/10.1016/j.cma.2013.01.011

[24] H. Esterbauer, K. H. Cheeseman, [42] determination of aldehydic lipid peroxidation products: Malonaldehyde and 4-hydroxynonenal, Methods in enzymology 186 (1990) 407–421.

[25] V. Katalinic, D. Modun, I. Music, M. Boban, Gender differences in antioxidant capacity of rat tissues determined by 2,2'-azinobis (3-ethylbenzothiazoline 6-sulfonate; ABTS) and ferric reducing antioxidant power (FRAP) assays., Comp Biochem Physiol C Toxicol Pharmacol 140 (1) (2005) 47–52. http://doi.org/10.1016/j.cca.2005.01.005

[26] ANKOM Methods, Method for Crude Fat Determinations, ANKOM Technology Corporation, Macedon, NY (2001).

[27] F. H. Lesh, Multi-dimensional least-squares polynomial curve fitting, Communications of the Acm 2 (9) (1959) 29–30.

[28] F. El Halabi, D. Gonzalez, A. Chico, M. Doblare, Fe2 multiscale in linear elasticity based on parametrized microscale models using proper generalized decomposition, Comput Meth Appl Mech Eng 257 (2013a) 183–202. https://doi.org/10.1016/j.cma.2013.01.011

[29] M. Sierra, J. Grasa, M.J. Muñoz, F.J. Miana-Mena, D. González, Predicting muscle fatigue: a response surface approximation based on proper generalized decomposition technique, Biomech Model Mechanobiol. 16 (2) (2017) 625-634. http://dx.doi.org/10.1007/s10237-016-0841-y

[30] A. Ammar, B. Mokdad, F. Chinesta, R. Keunings, A new family of solvers for some, classes of multidimensional partial differential equations encountered in kinetic theory modeling of complex fluids, J Non-Newton Fluid 139 (3) (2006) 153–176. https://doi.org/10.1016/j.jnnfm.2006.07.007

[31] A. Ammar, B. Mokdad, F. Chinesta, R. Keunings, A new family of solvers for some classes of multidimensional partial differential equations encountered in kinetic theory modelling of complex fluids: Part ii: Transient simulation using space-time separated representations, J Non-Newton Fluid 144 (2–3) (2007) 98–121. https://doi.org/10.1016/j.jnnfm.2007.03.009

[32] A. Nouy, A generalized spectral decomposition technique to solve a class of linear stochastic partial differential equations. Comput Meth Appl Mech Eng 196(45–48) (2007) 4521–4537. https://doi.org/10.1016/j.cma.2007.05.016.

[33] F. Chinesta, A. Leygue, F. Bordeu, J.V. Aguado, E. Cueto, D. Gonzalez, I. Alfaro, A. Ammar, A. Huerta, Pgd-based computational vademecum for efficient design, optimization and control. Arch Comput Method Eng 20(1) (2013) 31–59.

[34] S. Niroomandi, D. González, I. Alfaro, F. Bordeu, A. Leygue, E. Cueto, F. Chinesta, Real-time simulation of biological soft tissues: a PGD approach, Int. J. Numer. Meth. Biomed. 29 (5) (2013) 586–600. http://dx.doi.org/10.1002/cnm.2544

[35] D. González, E. Cueto, F. Chinesta, Real-time direct integration of reduced solid dynamics equations, Int. J. Numer. Methods Eng. 99 (9) (2014) 633–653.

http://dx.doi.org/10.1002/nme.4691

[36] A. Leygue, E. Verron, A first step towards the use of proper general decomposition method for structural optimization, Archives of Computational Methods In Engineering 17 (4) (2010) 465–472. http://dx.doi.org/10.1007/s11831-010-9052-3

[37] B. Bahloul, M. A. Lassoued, S. Sfar, A novel approach for the development and optimization of self emulsifying drug delivery system using hlb and response surface methodology: application to fenofibrate encapsulation, International journal of pharmaceutics 466 (1) (2014) 341–348. http://dx.doi.org/10.1016/j.ijpharm.2014.03.040

[38] F. C. B. C. de Melo, D. Borsato, F. C. de Macedo, C. Celligoi, Study of levan productivity from bacillus subtilis natto by surface response methodology and its antitumor activity against hepg2 cells using metabolomic approach, Pak. J. Pharm. Sci 28 (6) (2015) 1917–1926.

[39] R. D. C. Soltani, S. Jorfi, M. Safari, M.-S. Rajaei, Enhanced sonocatalysis of textile wastewater using bentonite-supported zno nanoparticles: Response surface methodological approach, Journal of environmental management 179 (2016) 47–57.

[40] S. Honary, P. Ebrahimi, R. Hadianamrei, Optimization of particle size and encapsulation efficiency of vancomycin nanoparticles by response surface methodology, Pharmaceutical development and technology 19 (8) (2014) 987–998. URL http://dx.doi.org/10.3109/10837450.2013.846375

[41] Z. Gasparova, O. Ondrejickova, A. Gajdosikova, A. Gajdosik, V. Snirc, S. Stolc, Oxidative stress induced by the Fe/ascorbic acid system or model ischemia in vitro: effect of carvedilol and pyridoindole antioxidant SMe1EC2 in young and adult rat brain tissue., Interdiscip Toxicol 3 (4) (2010) 122–126. http://dx.doi.org/10.2478/v10102-010-0051-x

[42] W. Zheng, A. D. Monnot, Regulation of brain iron and copper homeostasis by brain barrier systems: implication in neurodegenerative diseases., Pharmacol Ther 133 (2) (2012) 177–188. http://doi.org/10.1016/j.pharmthera.2011.10.006

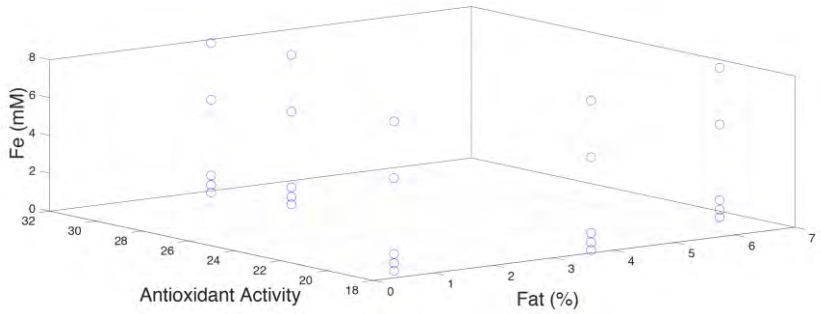

Fig. 1

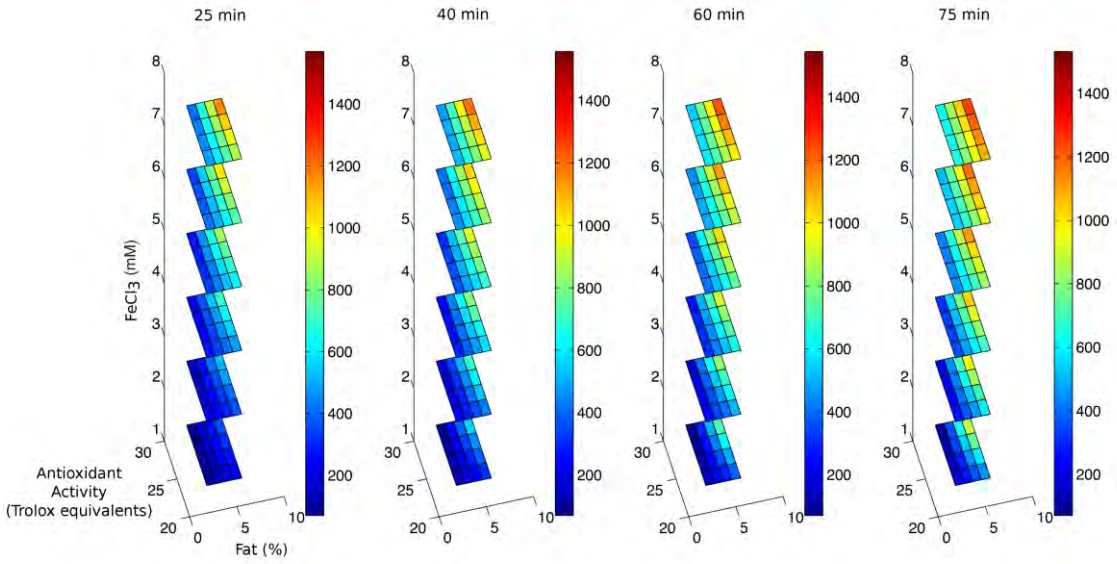

Fig. 2

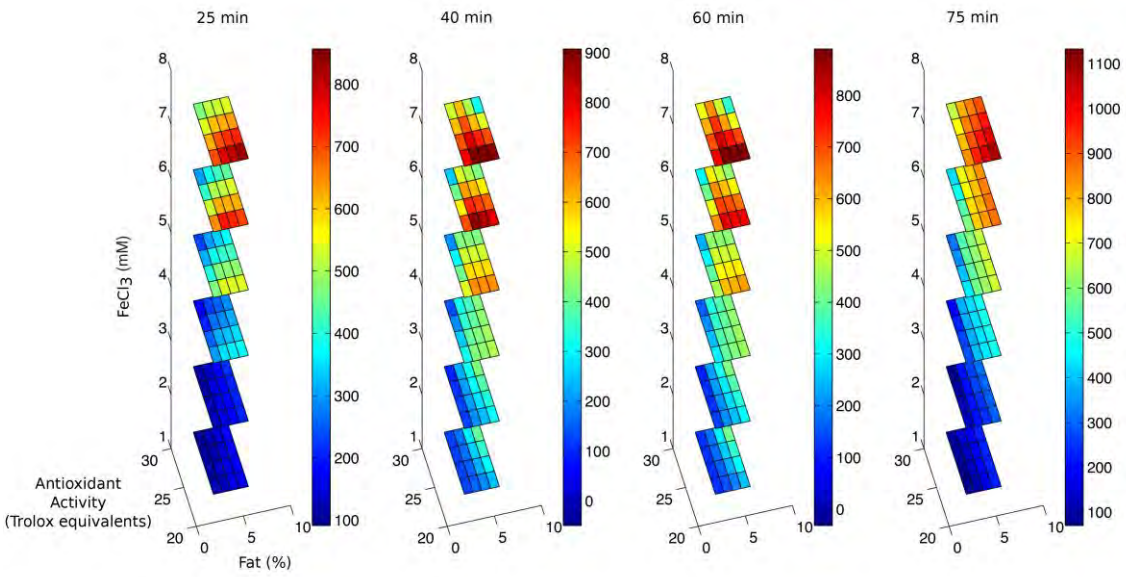

Fig. 3

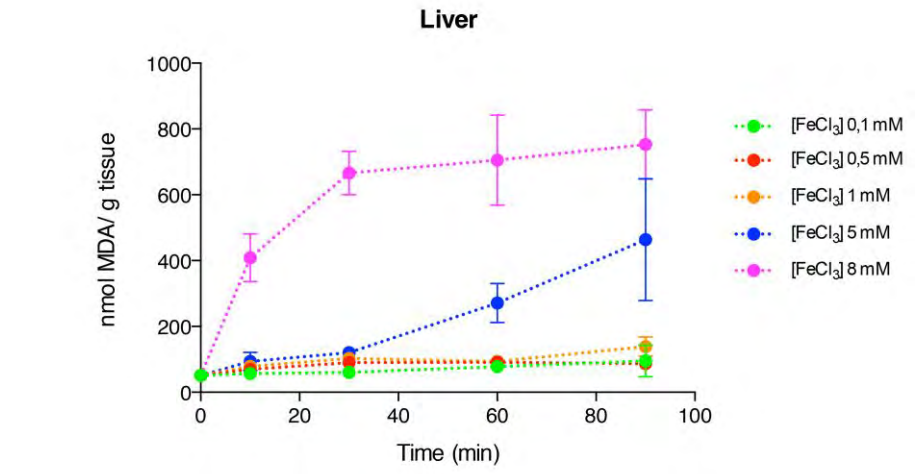

A

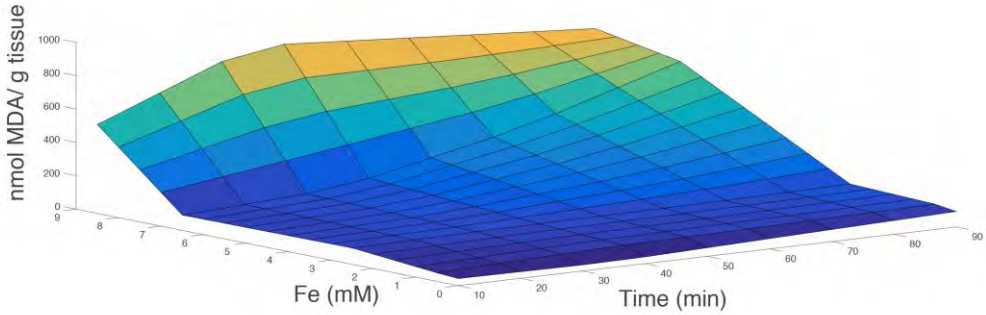

B

Fig. 4

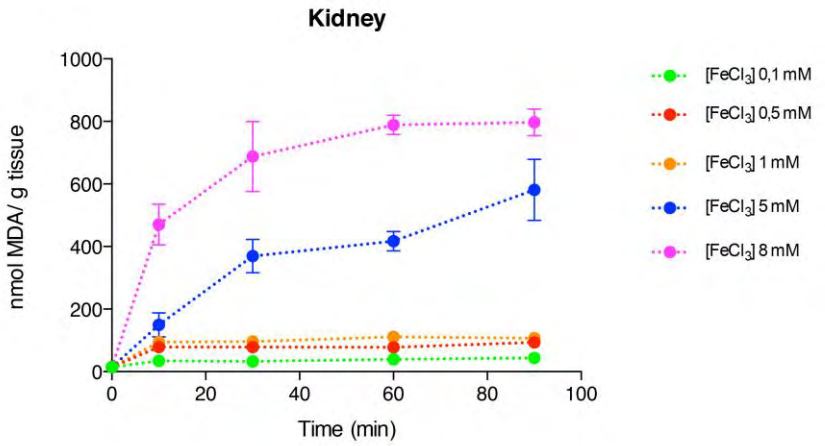

A

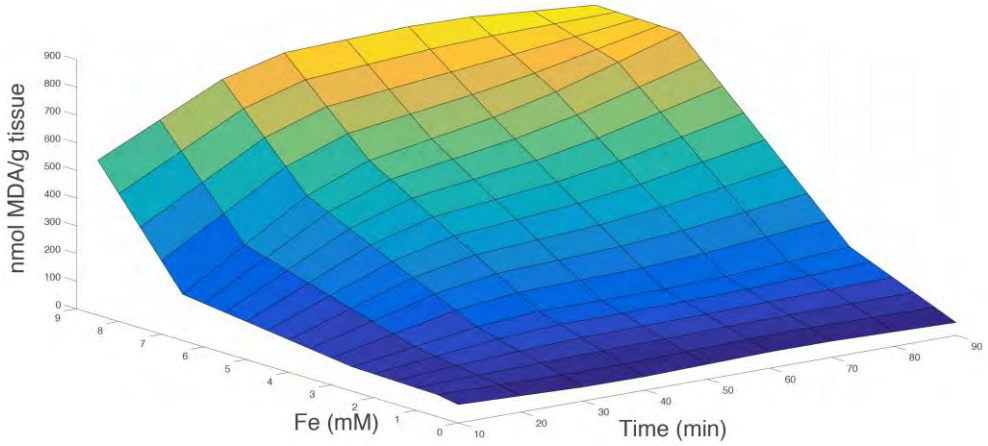

B

Fig. 5

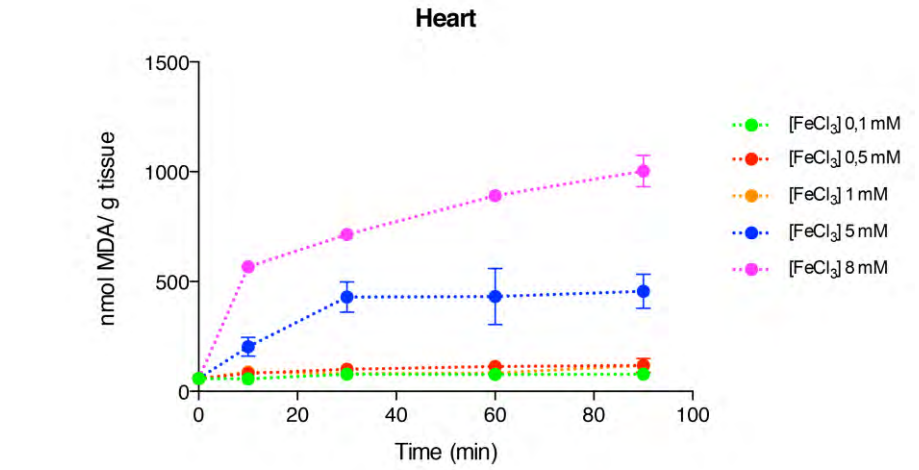

A

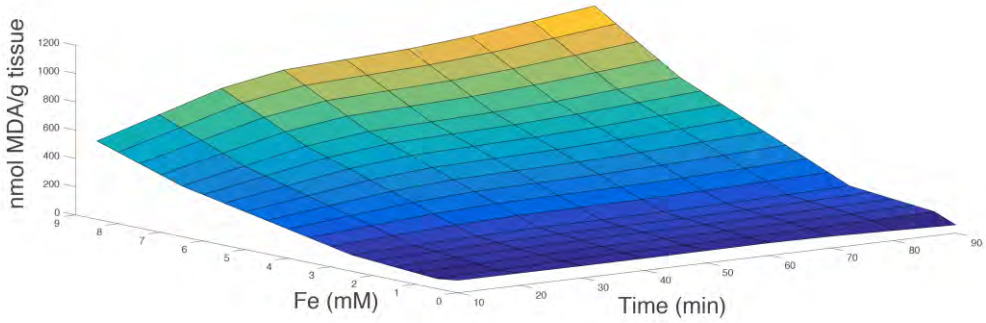

B

Fig. 6

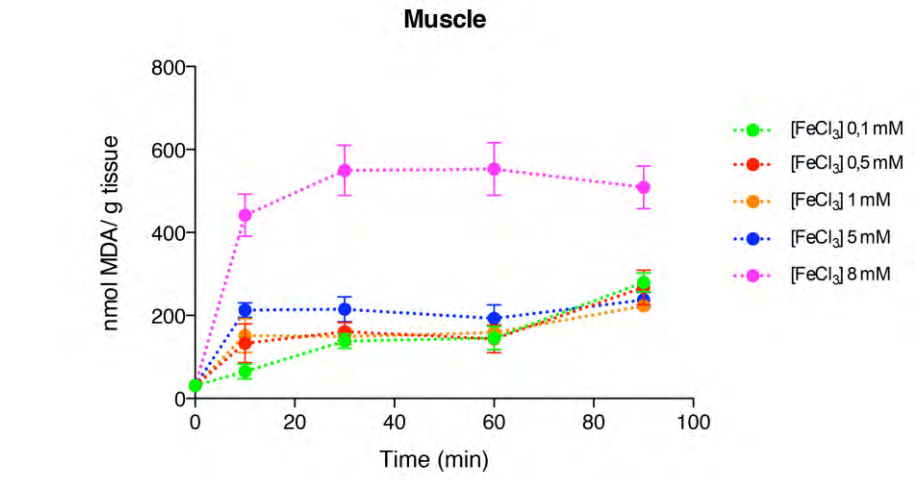

A

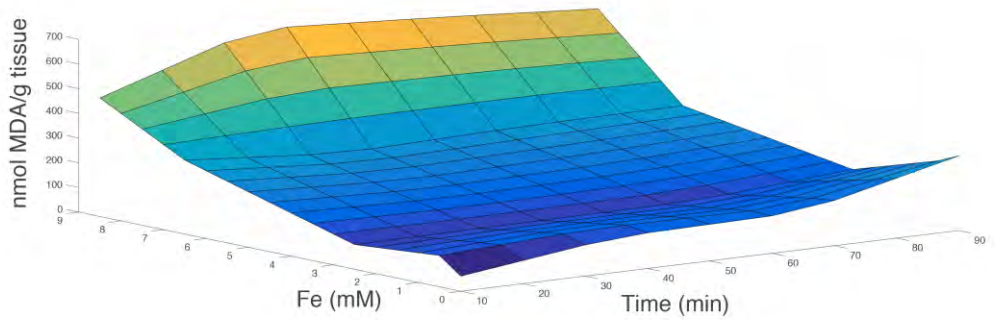

B

Fig. 7

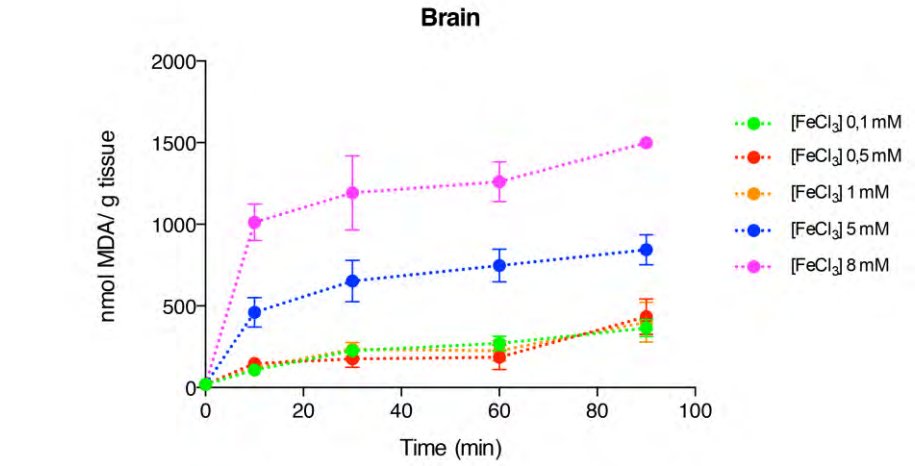

A

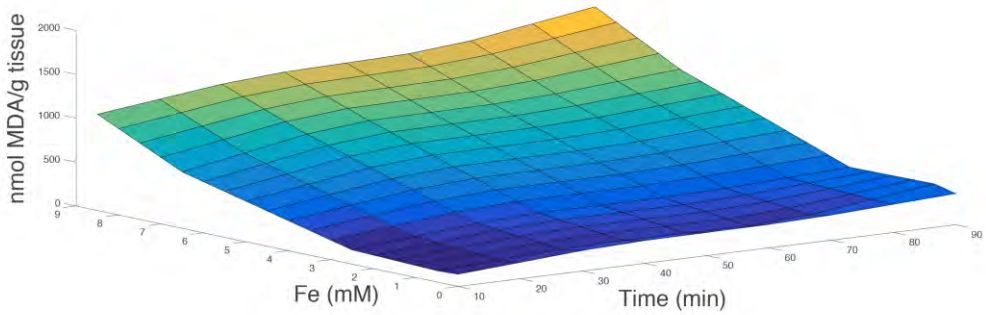

B

Fig. 8

Table 1: Fat composition and antioxidant activity of the different organs. Lung values were not used to build the response surface but to check its ability to predict MDA + 4-HDA concentration.

Organ	Fat Composition ± SD (%)	Antioxidant Activity ± SD (Trolox equivalents)
Liver	2.49 ± 0.105	31.52 ± 1.43
Kidney	2.75 ± 0.037	28.72 ± 0.36
Brain	6.6 ± 0.116	20.24 ± 1.14
Skeletal Muscle	0.58 ± 0.02	18.10 ± 1.48
Heart	3.66 ± 0.065	18.63 ± 1.44
Lung	2.99 ± 0.06	24.8 ± 2.27

Organ	$FeCl_3$ (mM)	Time (min)	Average experimental data MDA (nmol/g of tissue)	Predicted MDA (nmol/g of tissue)	Deviation (%)
Liver	0.5	30	90.6	76.1	15.9
	5.0	30	120.5	122.5	1.7
	8.0	30	666.0	649.3	2.5
	5.0	90	464.1	461.8	0.5
	8.0	90	753.2	732.1	2.8
Kidney	0.5	30	78.6	70.9	9.7
	5.0	30	369.4	335.8	9.1
	8.0	30	688.1	690.2	0.3
	5.0	90	581.1	574.4	1.1
	8.0	90	797.3	802.7	0.7
Heart	0.5	30	100.6	87.9	12.6
	5.0	30	428.8	386.7	9.8
	8.0	30	714.3	748.6	4.8
	5.0	90	455.4	507.7	11.5
	8.0	90	1002.6	990.6	1.2
Muscle	0.5	30	161.2	153.0	5.1
	5.0	30	215.2	201.2	6.5
	8.0	30	549.9	546.3	0.6
	5.0	90	237.6	230.8	2.9
	8.0	90	508.7	515.0	1.2
Brain	0.5	30	175.8	196.3	11.7
	5.0	30	651.8	669.1	2.7
	8.0	30	1193.1	1172.0	1.8
	5.0	90	844.6	844.1	0.1
	8.0	90	1498.7	1490.2	0.6

Table 2: Numerical test for input data used initially for the computation of the response surface particularized at liver, kidney, heart, muscle and brain. Predicted values are obtained from Eq. 2, after the inclusion of specific values of each organ.

Organ	$FeCl_3$ (mM)	Time (min)	Average experimental Data MDA (nmol/g of tissue)	Predicted MDA (nmol/g of tissue)	Deviation (%)	Melatonin (mM)
Lung	0.5	30	91.3	100.26	9.8	-
	1.0	30	111.0	118.4	6.7	-
Kidney	0.5	30	61.1	70.2	14.9	0.5
	0.5	30	57.9	59.3	2.4	0.8

Table 3: Numerical test for the validation of the response surface. Lung data used for the validation, with AA = 24**:** 8 (Trolox equivalents) and fat = 2**:** 99 (%). Kidney with melatonin lipid peroxidation and AA data not used initially for the computation of the response surface, and fat = 2**:** 75 (%).

Oxidative stress prediction: a preliminary approach using a response surface based technique

HIGHLIGHTS

- A response surface is proposed to predict in vitro lipid peroxidation of any organs.
- Biological data were required to build the response surface (mathematical model).
- Lipid peroxidation level of rabbit tissues was measured in a $FeCl_3$/ascorbate model.
- Fat content and antioxidant capacity of rabbit tissues were determined.
- Response surface carried out accurate predictions of lipid peroxidation levels.